AD-A191 410 IMPLICATIONS OF THE TRAPPING-DESORPTION AND DIRECT INELASTIC SCATTERING C..(U) AEROSPACE CORP EL SEGUNDO CA CHEMISTRY AND PHYSICS LAB R P FRUEHOLZ ET AL. 1/1

UNCLASSIFIED 12 FEB 88 TR-0086(6945-05)-7 SD-TR-88-31 F/G 20/3 NL

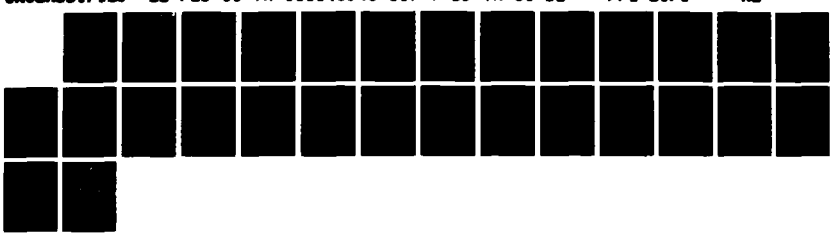

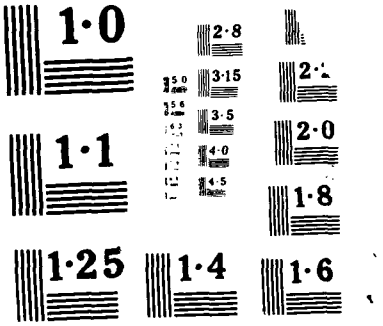
1·0
1·1
1·25
1·4
1·6
1·8
2·0
2·8
3·15
3·5
4·0
4·5

REPORT SD-TR-88-31

Implications of the Trapping-Desorption and Direct Inelastic Scattering Channels on Dicke-Narrowed Lineshapes

R. P. FRUEHOLZ and J. C. CAMPARO
Chemistry and Physics Laboratory
The Aerospace Corporation
El Segundo, CA 90245

Prepared for

SPACE DIVISION
AIR FORCE SYSTEMS COMMAND
Los Angeles Air Force Base
P.O. Box 92960, Worldway Postal Center
Los Angeles, CA 90009-2960

This report was submitted by The Aerospace Corporation, El Segundo, CA 90245, under Contract No. F04701-85-C-0086 with the Space Division, P.O. Box 92960, Worldway Postal Center, Los Angeles, CA 90009-2960. It was reviewed and approved for The Aerospace Corporation by S. Feuerstein, Director, Chemistry and Physics Laboratory.

Lt Michael J. Mitchell was the project officer for the Mission-Oriented Investigation and Experimentation (MOIE) Program.

This report has been reviewed by the Public Affairs Office (PAS) and is releasable to the National Technical Information Service (NTIS). At NTIS, it will be available to the general public, including foreign nationals.

This technical report has been reviewed and is approved for publication. Publication of this report does not constitute Air Force approval of the report's findings or conclusions. It is published only for the exchange and stimulation of ideas.

Michael J. Mitchell

MICHAEL J. MITCHELL, Lt, USAF
MOIE Project Officer
SD/CWNZS

Raymond M. Leong

RAYMOND M. LEONG, Major, USAF
Deputy Director, AFSTC West Coast Office
AFSTC/WCO OL-AB

UNCLASSIFIED
SECURITY CLASSIFICATION OF THIS PAGE

REPORT DOCUMENTATION PAGE

1a REPORT SECURITY CLASSIFICATION Unclassified	1b. RESTRICTIVE MARKINGS
2a. SECURITY CLASSIFICATION AUTHORITY	3. DISTRIBUTION / AVAILABILITY OF REPORT Approved for public release; distribution unlimited.
2b. DECLASSIFICATION / DOWNGRADING SCHEDULE	
4. PERFORMING ORGANIZATION REPORT NUMBER(S) TR-0086(6945-05)-7	5. MONITORING ORGANIZATION REPORT NUMBER(S) SD-TR-88-31
6a. NAME OF PERFORMING ORGANIZATION The Aerospace Corporation Laboratory Operations 6b. OFFICE SYMBOL (If applicable)	7a. NAME OF MONITORING ORGANIZATION Space Division
6c. ADDRESS (City, State, and ZIP Code) El Segundo, CA 90245	7b. ADDRESS (City, State, and ZIP Code) Los Angeles Air Force Base Los Angeles, CA 90009-2960
8a. NAME OF FUNDING / SPONSORING ORGANIZATION 8b. OFFICE SYMBOL (If applicable)	9. PROCUREMENT INSTRUMENT IDENTIFICATION NUMBER F04701-85-C-0086-P00016
8c. ADDRESS (City, State, and ZIP Code)	10. SOURCE OF FUNDING NUMBERS PROGRAM ELEMENT NO. / PROJECT NO. / TASK NO. / WORK UNIT ACCESSION NO.

11. TITLE (Include Security Classification)
Implications of the Trapping-Desorption and Direct Inelastic Scattering Channels on Dicke-Narrowed Lineshapes

12. PERSONAL AUTHOR(S)
Frueholz, R. P. and Camparo, J. C.

13a. TYPE OF REPORT	13b. TIME COVERED FROM ____ TO ____	14. DATE OF REPORT (Year, Month, Day)	15. PAGE COUNT
		1988 February 12	24

16. SUPPLEMENTARY NOTATION

17 COSATI CODES			18. SUBJECT TERMS (Continue on reverse if necessary and identify by block number)
FIELD	GROUP	SUB-GROUP	Atomic Storage Cells Hydrogen adsorption Microwave spectroscopy Atomic physics

19. ABSTRACT (Continue on reverse if necessary and identify by block number)

The Dicke-narrowed lineshape of an atom in a wall-coated, bufferless, atomic storage cell is composed of two parts, a sharp central spike and a broad underlying pedestal. To understand the pedestal shape, we find that it is necessary to account for various atom-surface scattering channels. Conversely, analysis of the pedestal shape yields information concerning these scattering channels. In particular, nearly Doppler-broadened pedestals, observed for alkali hyperfine transitions in cells with paraffin coatings, indicate that both a trapping-desorption channel and a direct inelastic/quasi-elastic channel are accessible in the atom-surface scattering process. Alternatively, the appearance of much narrower pedestals, observed in cells with dichlordimethylsilane coatings, indicates that the trapping-desorption channel dominates the atom-surface scattering process.

20. DISTRIBUTION / AVAILABILITY OF ABSTRACT ☒ UNCLASSIFIED/UNLIMITED ☐ SAME AS RPT ☐ DTIC USERS	21. ABSTRACT SECURITY CLASSIFICATION Unclassified
22a. NAME OF RESPONSIBLE INDIVIDUAL	22b. TELEPHONE (Include Area Code) / 22c. OFFICE SYMBOL

DD FORM 1473, 84 MAR 83 APR edition may be used until exhausted
All other editions are obsolete

SECURITY CLASSIFICATION OF THIS PAGE
UNCLASSIFIED

PREFACE

The authors wish to thank Mr. S. Delcamp for his assistance in performing the experiments, and Mr. R. Cook for fabricating the atomic storage cells.

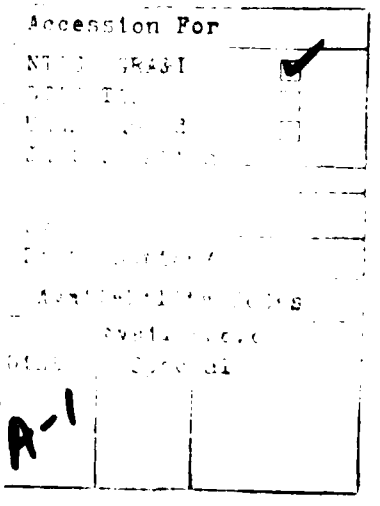

CONTENTS

FIGURES

I. INTRODUCTION

In microwave spectroscopy one often encounters situations in which the atomic or molecular dephasing times are very long, so that collisions of gas phase atoms with the walls of a storage vessel have a non-negligible influence on the observed lineshape. In one extreme, where the storage vessel's surfaces are strongly depolarizing, the atom-surface impacts produce a discontinuous change in the phase of the atomic oscillator, and this results in an additional broadening of the homogeneous linewidth by an amount proportional to the rate of atom-surface collisions.[1,2] The details of the atom-surface interaction are in this case lost, and the lineshape simply depends on the geometry of the storage vessel. However, if the storage vessel's surfaces are weakly depolarizing, then the atom-surface interaction potential, which perturbs the atomic system for some brief period of time, results in a shift of the atomic resonance frequency.[3,4] Additionally, if the dimensions of the storage vessel are less then the wavelength of the radiation, so that Dicke's criterion is satisfied,[5] motional narrowing of the Doppler broadened lineshape occurs (it will be shown below how this "Dicke" narrowing is also sensitive to the atom-surface interaction). Thus, in the case of a weakly depolarizing surface, the nature of the atom-surface interaction is manifested in the observed lineshape, and one might expect the study of atomic lineshapes in such storage vessels to provide a fruitful melding of surface and atomic physics.

Investigations of atom-surface interactions, while traditionally the realm of the surface scientist, have more recently begun to draw heavily on techniques developed in other areas of physics, particularly atomic physics. Specifically, atom-surface interactions are now often studied directly by scattering well collimated, nearly monoenergetic atomic beams from various surfaces. Energy and angular analysis of the scattered atoms provide insights into the different scattering channels accessible to the incident atoms.[6,7] The relaxation of optically pumped atoms, investigated through the use of optically (laser) prepared and analyzed atomic beams, also directly probes the

atom-surface interactions.[8] In addition to contributing to techniques which allow direct study of atom-surface interactions, various experiments in atomic physics have indirectly probed these interactions. Experiments investigating the relaxation of spin polarized alkali atoms in storage cells with weakly depolarizing cell walls have shed light on aspects of the alkali adsorption process.[9-11] The interaction of hydrogen atoms with a fairly complicated surface, teflon, have been probed through a study of the frequency shifts in a hydrogen maser,[3] the results of which yielded insights into hydrogen adsorption and energy accommodation as well as teflon surface structure. In fact, Zitzewitz and Ramsey,[3] recognizing the symbiotic relationship between surface science and atomic physics, suggested that "the hydrogen maser can be used as an experimental tool to study atom-surface interactions, albeit indirectly." In this report the relationship between surface science and atomic physics is further elucidated. Specifically, we show that motionally or "Dicke"-narrowed atomic hyperfine lineshapes in wall-coated, bufferless atomic storage cells cannot be properly understood without a consideration of the appropriate atom-surface scattering channels, and that consequently these lineshapes yield significant information concerning the atom-surface scattering process.

Dicke (or collisional) narrowing in an atomic transition results in a lineshape with a spectral width less than the Doppler width,[5,13] and it is observed when atoms are confined to small volumes of space through rapid velocity changing collisions. In order to observe this phenomenon, the atomic mean free path must be less than the wavelength of the atomic resonance under study. Additionally, the phase of the interrogating field must remain constant within the confinement region, and if this requirement is not satisfied, an additional broadening of the observed lineshape occurs.[14] A final constraint for observation of the phenomenon requires the confining collision to be non-perturbing, that is, the internal state of the atom must be unchanged by the confining collisions. The implications of this last requirement in the context of the present study will be discussed subsequently. In the study of alkali ground state hyperfine transitions, where the transition wavelength is on the order of centimeters, atomic

confinement can be obtained through use of an inert buffer gas or by placing the radiating atoms in an evacuated cell with a non-relaxing surface. When the atom's spatial confinement results from collisions with the storage vessel's walls, the narrowed lineshape is composed of two components, a Doppler-free central spike whose width is determined by the various relaxation processes occurring within the storage vessel, and a broad underlying pedestal with a width typically found to be approximately equal to the Doppler width.[5,13,14] However, the present analysis shows that the interactions between interrogated atoms and storage cell surfaces are crucial for determining the pedestal shape.

Weinberg and Merrill[15] have discussed three different scattering channels that are potentially accessible to an atom when it impacts a surface with a near-thermal speed. The atom may rebound "quasi-elastically" with very little energy transfer between itself and the surface; a "direct inelastic" scattering channel may be open, in which there is significant energy transfer between the atom and the surface; or lastly, the atom may scatter from the surface through a "trapping desorption" channel in which the atom is physically adsorbed to the surface and subsequently, after full energy accomodation, desorbs. In an elegant series of beam studies, Hurst et al.[16-18] investigated the accessible scattering channels for various rare gases impacting clean metallic surfaces such as platinum (111) and polycrystalline tungsten. In their studies atoms which underwent trapping-desorption could be clearly separated from those which underwent direct inelastic scattering.

The characteristics Hurst et al. found for each of these channels can be briefly summarized. In the direct inelastic channel, the incident atom interacts with the surface for a vry short period of time compared to the residence time associated with trapping-desorption.[6,17] (Surface residence time is important, since atomic spin or hyperfine polarization relaxation in an evacuated cell is due to atom-surface magnetic interactions; the longer an atom is in the vicinity of the surface the greater the surface's perturbation of the atom's internal state.) The angular nature of the direct-inelastic channel was found to be highly specular, and energetically was relatively

elastic, leading to a correlation between incident and exit atomic speeds. Furthermore, for Ar scattering from polycrystalline tungsten, when the incident Ar atoms displayed a Maxwell-Boltzmann speed distribution appropriate to the surface's temperature, the atoms that were scattered through the direct-inelastic channel displayed a speed distribution richer in high velocities. Considering the quasi-elastic scattering channel, one would expect the specular and elastic nature of the scattering to be even more stringent than in the case of the direct inelastic channel. With regard to trapping-desorption, in addition to relatively long surface residence times, this channel was found to be characterized by a high degree of energy exchange between the adsorbed atom and the surface. In the specific case of Ar scattering from tungsten, Hurst et al. found that the emission angular distribution was broader than cosine, that is, with more atoms at large angles relative to the surface normal. Additionally, the observed emission speed distribution was found to be deficient in high velocities relative to a Maxwell-Boltzmann speed distribution appropriate to the surface temperature. They also observed that the probability of trapping-desorption could be enhanced if incident atoms had low energies or approached the surface at a grazing angle.

Generalizing these results to vapor phase atoms confined by a spherical storage vessel, one may say that an atom scattering through the trapping-desorption channel should have a lower average emission energy than that expected from a Maxwell-Boltzmann distribution specified by the surface temperature, and that the greater than cosine probability of large-angle emission will enhance the possibility of subsequent grazing collisions. Consequently, once an atom scatters through the trapping-desorption channel, the probability of a subsequent trapping-desorption scattering event is increased. In the same vein, the fairly elastic nature and potentially higher than expected (from surface temperature considerations) emission energies associated with the direct inelastic channel, favor subsequent direct inelastic scattering events after an atom has initially scattered through this channel. For the present work then, the important conclusion to be drawn is that in the gas phase, atoms initially associated with either a trapping-desorption channel or a direct inelastic channel appear to display a strong propensity to remain associated with that particular channel.

II. THEORETICAL ANALYSIS AND RESULTS

Motional narrowing in evacuated wall coated cells was first addressed by Dicke[5] when he analyzed the spectrum of the radiation emitted by an atom in a one-dimensional box. Frueholz and Volk[13] generalized Dicke's analysis to the three-dimensional case of radiating atoms in spherical storage cells, and in a two-part analysis they specifically analyzed the hyperfine lineshape of a Rb^{87} atom confined in a bufferless cell with a nonrelaxing surface. In their analysis, the trajectories of a single atom within the storage cell are calculated using a Monte Carlo technique. The resulting trajectory yields the times between wall collisions as well as the Doppler-shifted frequency of the radiation emitted by the atom. Within the Monte Carlo portion of the analysis, many properties of the atom-surface interaction, as just described, may be incorporated. After generation of the atomic trajectories, the analysis of Frueholz and Volk treated the polarized atom as a classical radiator and the emitted wavetrain was Fourier analyzed to yield the Dicke narrowed lineshape. The lineshapes so obtained consisted of a central spike, matching experiment, and a broad pedestal with a width well below the experimentally observed, approximately Doppler width. Despite extensive analysis, no satisfactory explanation for the discrepancy could be obtained. To remove any questions concerning the applicability of a classical lineshape analysis, the current study combines a density matrix approach with the Monte Carlo atomic trajectories to generate the Dicke-narrowed lineshapes. Specifically, the lineshape of the Rb^{87} 0-0 hyperfine transition for an atom in a spherical cell is analyzed. For simplicity the atom is treated as a two level system. We assume that depopulation pumping to an upper electronic level by frequency-selected light creates a population imbalance between the two levels, and a resonant microwave field is detected by a decrease in the optical-pumping light. This is an accurate representation of previously conducted experiments.[14]

The density matrix equations describing this system have been derived previously.[19] The three coupled differential equations, Eqs. (1a) - (1c),

describe the temporal evolution of one level's population, σ_{22}, and the real and imaginary parts of the system's coherence. The equations depend parametrically on the optical photon absorption rate B, the microwave Rabi frequency ω_1, the detuning of the microwave field from the atomic resonance frequency as perceived by the moving atom $\Delta(t)$ and phenomenological longitudinal and transverse surface relaxation rates $\gamma_1 = \gamma_2 = \gamma$. During traversal of the cell, γ is set equal to zero, but while the atom resides on the cell surface, γ assumes a nonzero value. The apparent detuning of the microwave field frequency from the atomic resonance frequency varies for each traversal due to differing Doppler shifts. As the differential equation coefficients change discretely only upon impact with the cell wall, and again upon reemission from the wall, the equations may be solved in closed form and the solution propagated from impact to reemission to impact etc. as the trajectory proceeds. The lineshape computation, performed on a computer, calculates the atomic trajectory over a period of time a factor of five greater than the inverse of the relaxation rates associated with the situation being studied. The initial conditions for the computation are $\sigma_{22} = 0.5$, and both the real and imaginary parts of the coherence are set equal to zero. As the lineshape resulting from this procedure is quite noisy, it is necessary to average several hundred such lineshapes. This requires the analysis of approximately 300,000 wall collisions. For simplicity, all calculations conducted have assumed that Rb^{87} atoms are emitted from the cell surface with a $\cos(\theta)$ distribution.

Our initial calculations assumed that all atoms were emitted from the surface with speeds distributed according to a single Maxwell-Boltzmann speed distribution. In light of the atom-surface scattering characteristics discussed previously, one would thus state that all the atoms were proceeding through the same surface-scattering channel. The optical pumping rate, microwave Rabi frequency, and wall relaxation rate were adjusted so that in the absence of atomic motion the hyperfine linewidth would be approximately 30 Hz. The residence time was taken to be 1×10^{-10}s, which is appropriate for the non-relaxing paraffin surface under consideration.[9,21] The wall relaxation rate was set at 1×10^{8}/s, and the calculations assumed a spherical

cell with a radius of 4 cm. When averaged over the time of flight between wall collisions, this wall relaxation rate thus contributed ~ 10 Hz to the motionless linewidth. It is worth noting that the absolute values of the wall residence time and the surface relaxation rate are not the physically important parameters in the present analysis. Rather, it is the product of the two, which specifies the amount of phase information lost upon each collision, which is important. We have, though, used physically realistic values for each quantity. The results of this calculation are shown in Fig. 1a. The central spike displays the expected linewidth; however, the pedestal is narrow with a width of 5.0 KHz, compared to the expected 9.2 KHz Doppler width. Just as in the classical Fourier analysis, a discrepancy between the experimentally observed pedestal[14] and the theoretical analysis is found.

It is reasonable to expect paraffin-coated glass surfaces to be relatively smooth on a microscopic scale. Long chain paraffin molecules will lie on the glass with their long axes parallel to the surface.[22] In addition, there may be a several monolayer thick coating of paraffin on the surface. Taken together, these factors would tend to reduce surface roughness. As a result, to reconcile experiment and theory, we feel it is reasonable to postulate that the atoms scatter from the surface through two different channels, a trapping-desorption (TD) channel and a direct inelastic/quasi-elastic (DI) channel. As a first step in taking into account the effects of the two scattering channels, we draw upon the well known concept of a critical speed for trapping S_c.[21] When an atom impinges upon a surface with a speed below S_c, indicating a low kinetic energy, simple analysis shows that it has a high probability of undergoing a TD scattering process (see Appendix). At the beginning of each of the several hundred lineshape calculations needed to generate a smooth hyperfine lineshape, an initial atomic speed is selected from a Maxwell-Boltzmann speed distribution. If this speed is below the critical speed for trapping, the atom is assumed to scatter initially and subsequently through the TD channel. Consequently, throughout a single lineshape calculation, the atom is only allowed to have speeds equal to or below S_c. Conversely, if the initial speed is above the critical speed for trapping, the atom scatters through the DI channel, and can therefore only

have speeds selected from the speed distribution that are equal to or above S_c. This procedure incorporates the observation that for a particular atom dual channel scattering is unlikely, and also provides a skewing of each channel's velocity distribution while maintaining an overall Maxwell-Boltzmann speed distribution. Additionally, if an atom scatters through the TD channel, it is provided with a longer, surface residence time. A simple analysis indicates that the TD atom-surface residence time was set fifty times greater than that of the DI channel (which was taken as 1×10^{-10}s). Thus, the only free parameter in this form of the calculation is S_c.

Using the same set of parameters that were used to generate Fig. 1a, we find that as S_c is increased, the pedestal broadens. This observation may be explained in a straightforward manner. When the scattering process is allowed to sample all speeds in the thermal distribution, the resulting pedestal width is less than the Doppler width, approximately 5 KHz. With the introduction of S_c, atoms that proceed through the DI channel sample higher speeds and display a higher effective "temperature" than those scattering off of the wall through the TD channel. Consequently, the pedestal due to atoms undergoing DI scattering will be broader than the normal thermal pedestal, while the converse holds for those atoms undergoing TD scattering. As S_c increases, both atomic populations "heat up", and the pedestal widths associated with the two groups of atoms increases. However, though the pedestal width of the DI group increases without bound, the pedestal width of the TD atoms is limited by the normal (~ 5 KHz) width.

The experimentally observed lineshape is the sum of the lineshapes due to both groups of atoms, and the magnitude of an individual group's lineshape depends on its fractional population as well as the degree of hyperfine polarization. The greater these quantites are, the larger a particular group's contribution to the total lineshape. Since the loss of hyperfine polarization that occurs upon each wall collision is proportional to the surface residence time associated with the impact, the degree of polarization for atoms scattering through the TD channel, with its relatively long residence time, is considerably less than it is for atoms interacting with the wall via the DI mechanism. Additionally, for reasonable values of S_c, a large

fraction of atoms are in the DI group. As a result, under certain conditions the observed lineshape will be dominated by DI atoms and the pedestal width will be greater than the normal thermal pedestal width. Of course the observed pedestal width cannot increase without limit. The fraction of atoms in the DI group drops rapidly as S_c increases beyond the average thermal speed. As a result, for very large values of S_c, the lineshape will be due primarily to those atoms proceeding through the TD channel, which (while displaying low polarization) comprise the major faction of all atoms. The resulting pedestal in this case would display the normal thermal width.

As discussed in the appendix, S_c is expected to be sensitive to both the atom-surface potential well depth D and the single impact energy accommodation coefficient α. In the appendix it is shown that a reasonable value for S_c is 1.8×10^4 cm/s (the most probable speed in our calculations is 2.9×10^4 cm/s). This yields the lineshape of Fig. 1b showing a 9.3 KHz wide (nearly Doppler width) pedestal, in excellent agreement with the pedestal reported by Robinson and Johnson.[14] While our method of including the effects of the two scattering channels in Dicke narrowing is admittedly simplistic, the theory's ability to match experiment with realistic input parameters provides strong evidence for two-channel scattering in the alkali atom/alkane surface system.

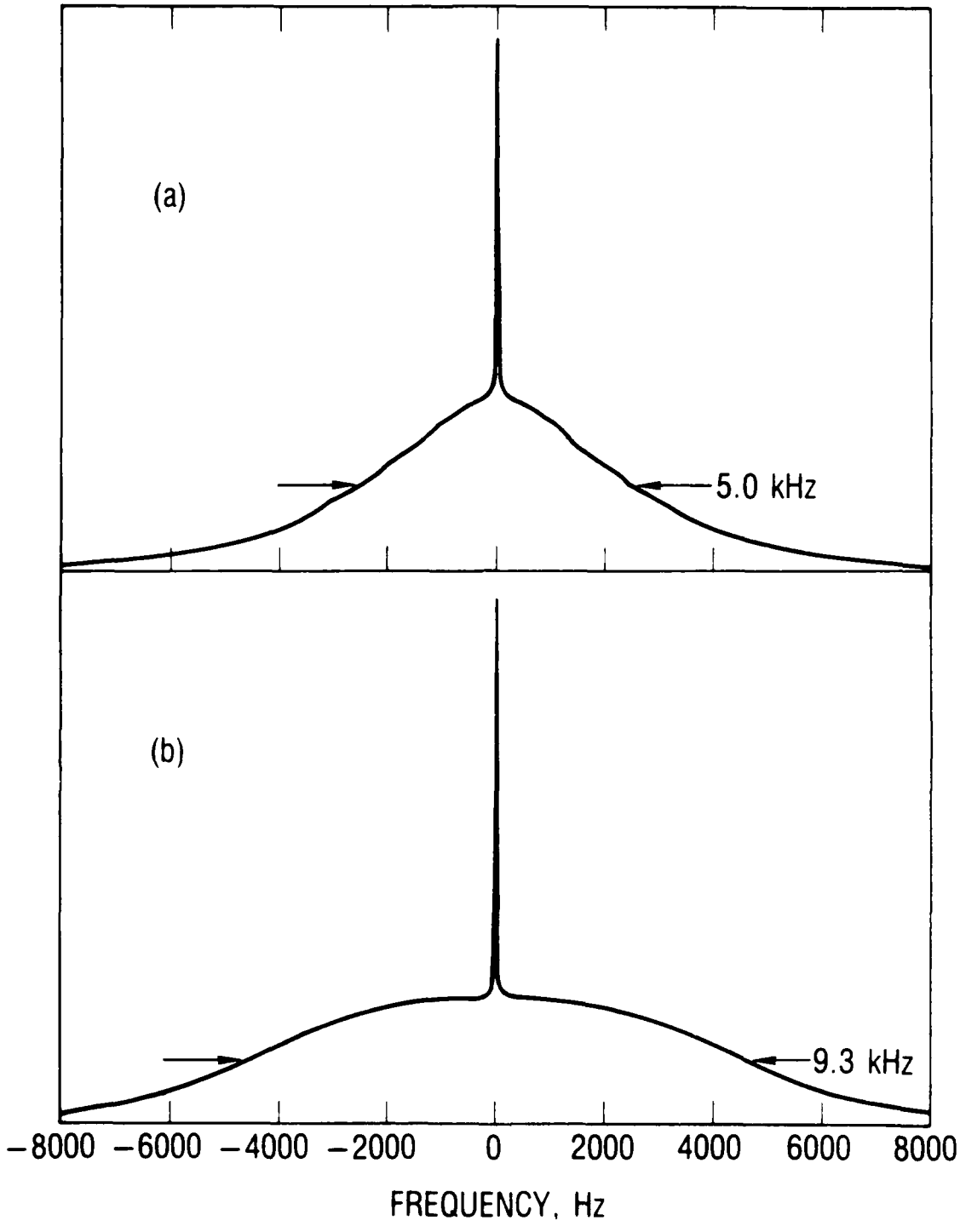

Fig. 1. Dicke-Narrowed Hyperfine Lineshapes for Rb^{87} in a 4.0 cm Radius Paraffin Coated, Bufferless Cell Obtained from the Trajectory/Density Matrix Analysis; the Hyperfine Linewidth in the absence of Atomic Motion is 30 Hz; (a) All Atoms Scatter Through a Single Channel, (b) Atoms Scatter Through Either a Trapping-Desorption or Direct Inelastic/Equasi-Elastic Channel.

III. EXPERIMENT

As a consequence of our analysis, if the atom-surface scattering proceeds exclusively through a single channel that has access to all speeds, the pedestal should assume the sub-Doppler shape of Fig. 1a; observation of such a Dicke-narrowed pedestal would run counter to all previous theoretical pedestal descriptions. The most reasonable situation for observing such a pedestal would be in a cell whose wall coating, while still non-relaxing, was "stickier" than paraffin; such a coating can be obtained by treating glass with dichlorodimethylsilane.[9,11] In a detailed series of studies, Camparo[22] investigated the properties of this coating material, and found the wall relaxation rate to be greater than that of paraffin due primarily to a longer ($> \times 100$) atomic residence time on the former surface. For this "sticky" surface, we would expect TD to be the dominant scattering channel, and S_c to be well above the average thermal speed. This allows, within our model, essentially all speeds to be accessed by a scattered atom, and the pedestal width would then be anticipated to be near the computed normal thermal width of approximately 5 KHz. To test this prediction, we have obtained a Dicke-narrowed Rb^{87} hyperfine transition lineshape from a cell with this wall coating.

Figure 2 shows the experimental arrangement. Light from a Sharp LT-026 MD single-mode diode laser, tuned to the D_2 resonance of Rb at 780.2 nm,[25] was collimated to a beam diameter of ~ 2.2 cm. The diode laser output power was approximately 1.6 mW, and its single-mode linewidth was 44 MHz. The spherical resonance cell was located inside a solenoid surrounded by three layers of mu-metal shielding, and was heated by a wire wound oven which maintained a thermal temperature gradient in the cell of some 30°C from the top to bottom; the oven wires were braided to minimize any extraneous oven magnetic field. A static magnetic field of a few gauss was produced by the solenoid in order to isolate the Rb^{87} 0-0 hyperfine transition. Microwave power was supplied to a microwave horn located inside the solenoid by a chain of rf multiplication and amplification. At the resonance cell, we estimate that the full microwave

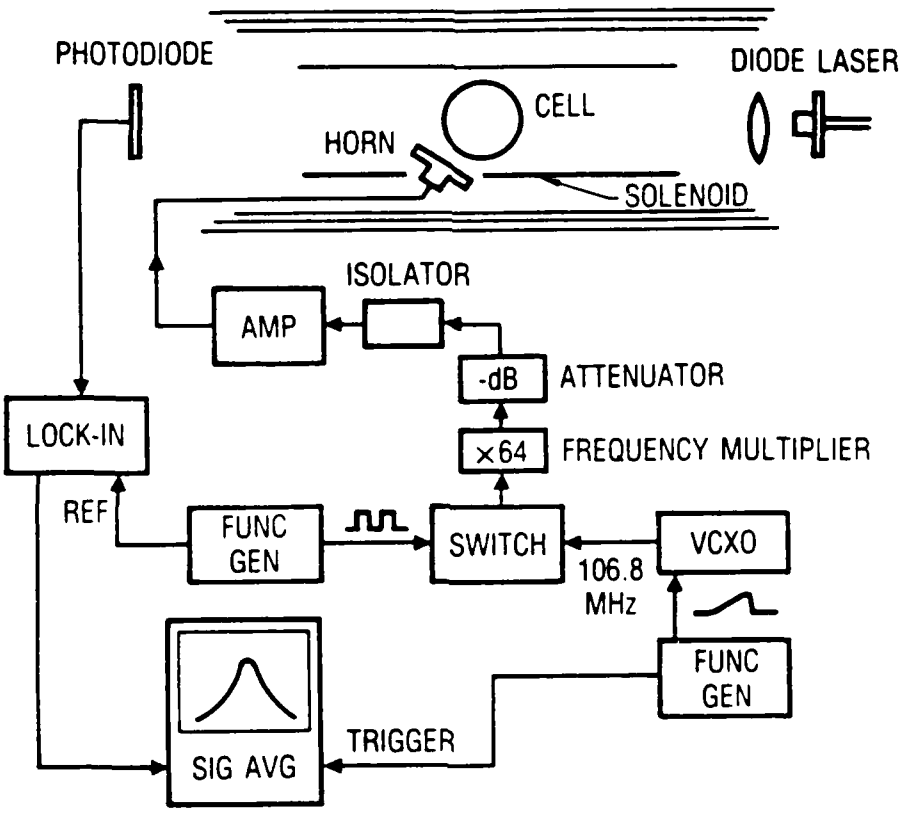

(a)

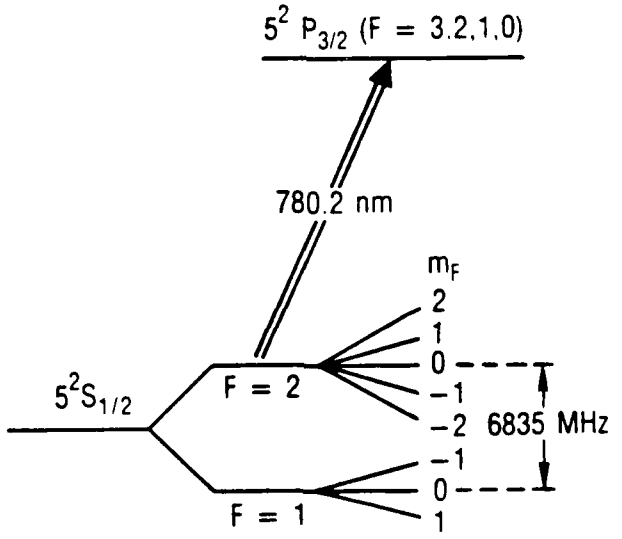

(b)

Fig. 2. (a) Optical Pumping Double Resonance Experimental Arrangement for Observing the Rb^{87} 0-0 Hyperfine Transition Lineshape. (b) Energy Level Diagram of Rb^{87} Showing the Atomic Transitions of Interest.

magnetic field strength in the absence of attenuation was roughly 14 mG. In order to employ phase sensitive amplification, the rf field was chopped prior to multiplication by a diode switch at a rate of ~ 70 Hz. Simultaneously, the frequency of the approximately 106.8 MHz rf coming from the voltage controlled crystal oscillator was ramped by a function generator, so that the microwave frequency swept slowly over the 0-0 hyperfine transition.

By tuning the diode laser to the D_2 Rb^{87} transition, the atomic population in the F=2 ground-state hyperfine manifold was transferred by depopulation pumping into the F=1 ground-state hyperfine manifold.[19] In the absence of microwaves at the appropriate frequency, this resulted in a maximum for the transmitted laser intensity. As the microwaves swept over the 0-0 hyperfine transition at 6835 MHz, atoms in the (F=1, m_F=0) ground-state Zeeman sublevel returned to the (F=2, m_F=0) ground-state Zeeman sublevel with the effect of reducing the diode laser transmitted intensity. The change in transmitted laser intensity as the microwaves swept across the resonance thus mapped out the 0-0 hyperfine transition lineshape. The transmitted intensity signal was phase-sensitive amplified by a lock-in amplifier, and stored in the memory of a signal averager. Because the microwave power had to be extremely low in order to avoid any possible microwave power broadening of the lineshapes (i.e. the microwave attenuator was set for 60 db), 1000 signal averages were required to obtain good signal-to-noise ratios for the experimental lineshapes.

The coating material was applied to the storage cell using the procedure of Zeng et al.[11] The cell contained a barium getter in an appendage to ensure that no impurity gas, which might have evolved within the cell after fabrication, would be present during the experiments. $\langle \vec{I} \cdot \vec{S} \rangle$ relaxation rate measurements after flashing the getter revealed that the dichlorodimethylsilane surface relaxation times were on the order of 530 μsec. This would imply that an average atom made the several velocity changing collisions required for Dicke-narrowing[13] before dephasing.

The experimentally observed lineshape is shown as the dashed curve in Fig. 3. Since the relaxation rates have broadened the central spike to a

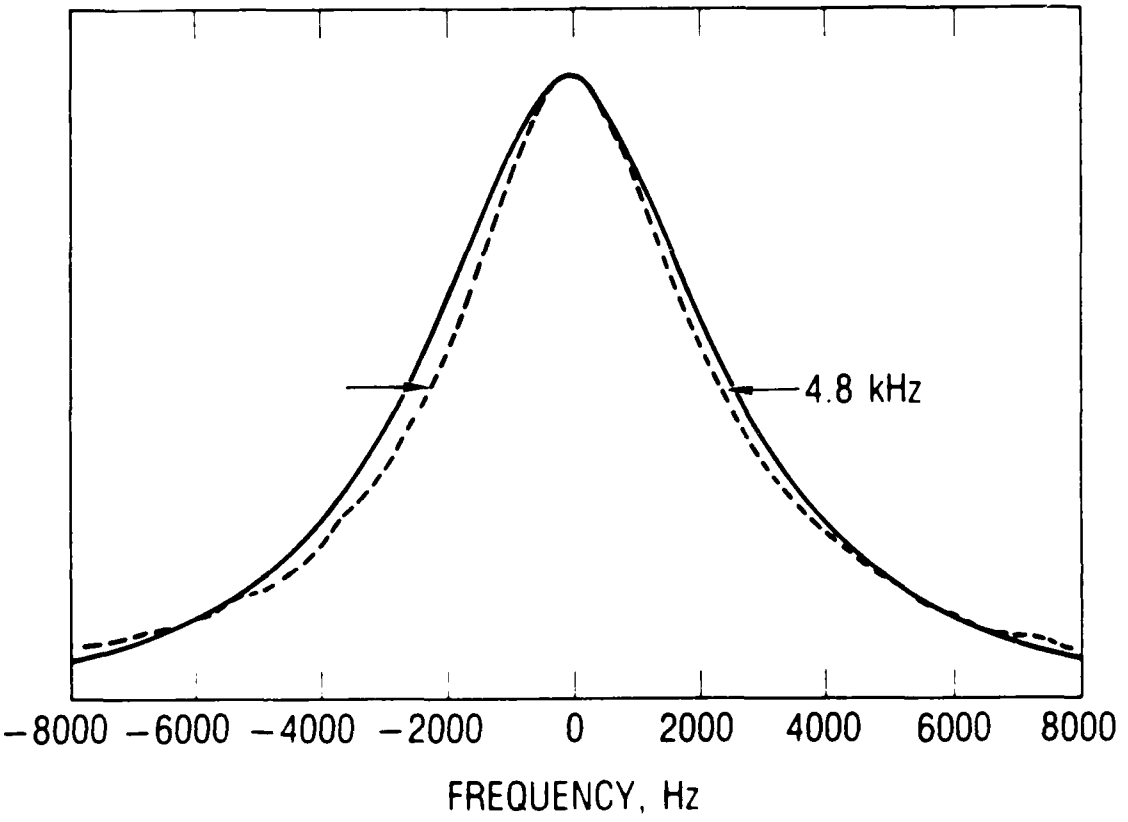

Fig. 3. Dicke-Narrowed Hyperfine Lineshapes for Rb^{87} in a 2.8 cm Radius Dichlorodimethylsilane-Coated Bufferless Cell. Dashed line experimental, solid line obtained from the trajectory/density matrix analysis. The hyperfine linewidth in the absence of motion is estimated to be approximately 1 KHz.

width of nearly 1 KHz, reducing its relative amplitude, the lineshape has the appearance of being exclusively due to the pedestal component. The observed linewidth is approximately 4.8 KHz with no hint of the spike. Using experimentally measured parameters for B, ω_1, and γ, and assuming that all scattering proceeds through a TD channel that now samples the entire Maxwell-Boltzmann speed distribution, our theoretical results normalized to the same maximum amplitude as experiment yield, the solid curve of Fig. 3 (FWHM 5.2 KHz). The excellent agreement with the experiment is consistent with our expectation of exclusive TD scattering. Additionally, to our knowledge, this is the first observation of a pedestal which is well below the generally expected Doppler width.

IV. DISCUSSION

The foregoing studies strongly suggest that in order to properly describe Dicke-narrowing in evacuated, wall-coated cells, it is necessary to take into account the atom-surface scattering process. Our theoretical analysis provides a means of testing the validity of specific models of the atom-surface interaction. If a model does not result in lineshapes matching experiment, it may be rejected. On the other hand, the ability to match experimental lineshapes does not unambiguously prove the validity of a particular model. This would require the preciseness of the much more complicated atomic beam-surface scattering experiments.

The models proposed, while admittedly simplistic and perhaps not correct in all specific aspects, do appear to correctly embody the major features of atom-surface scattering for the wall coating materials investigated. Specifically, in the presence of two scattering channels, the ensemble of polarized atoms should have a non Maxwell-Boltzmann speed distribution. The ensemble of polarized atoms in the presence of two-channel scattering is expected to be richer in high speeds compared to Maxwell-Boltzman speed distribution at the vapor temperature. Noting that the pedestal shape is influenced by the various polarized, atom Doppler shifts, one can for the first time rationalize the broad, approximately Doppler width, Dicke pedestals observed in the alkali atom/alkane surface. It would be worthwhile to experimentally validate the expectation of a non Maxwell-Boltzmann polarized atom speed distribution in the alkali atom/alkane surface system, since this would simultaneously provide a direct experimental measure of the critical speed for trapping, (which in the present lineshape theory is a free parametr). In the presence of a single scattering channel, the ensemble of polarized atoms has a Maxwell-Boltzmann speed distribution characterized by the vapor temperature, and under such conditions it is both theoretically predicted and experimentally observed that the Dicke pedestal is substantially narrower than the transition's Doppler width.

On a final note, it is worth mentioning that the present studies represent the first indication of two-channel scattering at thermal speeds in a system that would not be considered as clean in a traditional high vacuum sense. Thus, since Dicke narrowing predates the study of scattering channels, it would appear that evidence indicating the existence of various atom-surface scattering channels was available, but unrecognized, decades prior to their actual discovery.

APPENDIX

In the Dicke-narrowed lineshape theory discussed in the text, we employed the critical speed for trapping S_c[21,24] and used this speed to differentiate atoms which predominantly scattered through the TD channel from those which scattered mainly through the DI channel. In this appendix, we employ the simple atom-surface interaction model of Weinberg and Merrill[26] to indicate the manner in which the critical speed might be expected to depend on the physical properties of the atom-surface interaction.

Consider an atom of kinetic energy ε_i approaching a square well attractive potential with a well depth D. Just prior to impact with the repulsive part of the potential, the atom's initial kinetic energy is $E_i = D + \varepsilon_i$. Defining a single impact energy accommodation coefficient α in analogy with the standard thermal energy accommodation coefficient[25,26]

$$\alpha = \frac{E_i - E_f}{E_i - kT} \tag{A.1}$$

where E_f is the atom's kinetic energy after impact, and T is the surface temperature, we have

$$E_f = (1-\alpha)\,(D + mv_i^2/2) + \alpha kT \tag{A.2}$$

We can now define the critical speed for trapping in the following way: if $v_i \leq S_c$, then $E_f \leq D$ and the atom falls into the potential well and is consider "trapped". Thus, taking the limiting case and substituting S_c for v_i and D for E_f in Eq. (A.2)

$$S_c = \left[\frac{2\alpha\,(D-kT)}{m\,(1-\alpha)}\right]^{1/2} \tag{A.3}$$

or considering the ratio of S_c to the most probable thermal speed v_{mp},

$$S_c/v_{mp} = \left[\left(\frac{\alpha}{1-\alpha}\right)\left(\frac{D}{kT} - 1\right)\right]^{1/2} \qquad (A.4)$$

From the work of Bouchiat and Brossel[9] and Brewer[21], we approximate D for the alkali atom/alkane surface system as ~ 0.1 eV. Thus, to obtain S_c/v_{mp} = 0.62 (i.e., S_c = 1.8 × 10^4 cm/sec, which is the value used in the calculation for Fig. 1b), we require α = 0.12. The fact that this is a reasonable energy accommodation coefficient value[27,28] again suggests that the concept of two-channel scattering is valid in the alkali atom/alkane surface system.

REFERENCES

1. C. H. Townes and A. L. Schawlow, Microwave Spectroscopy (Dover, New York, 1975), p. 374.

2. M. Danos and S. Geschwind, Phys. Rev. 91, 1159 (1953).

3. P. W. Zitzewitz and N. F. Ramsey, Phys. Rev. A 3, 51 (1971).

4. If there is a non-zero variance in the average phase shift per impact, then a weakly depolarizing surface will also produce some homogeneous line broadening.

5. R. H. Dicke, Phys. Rev. 89, 472 (1953).

6. J. A. Barker and D. J. Auerbach, Surface Sci. Rep. 4, 1 (1985).

7. K. H. Rieder, Contemp. Phys. 26, 559 (1985).

8. P. R. Muessig and G. J. Diebold, Surf. Sci. 165, L 59 (1986).

9. M. A. Bouchiat and J. Brossel, Phys. Rev. 147, 41 (1966).

10. V. P. Putyrskii, Opt. Spectrosc. 41, 114 (1976).

11. X. Zeng, et al. Phys. Lett. 96A, 191 (1983).

12. R. P. Frueholz and C. H. Volk, J. Phys. B: At. Mol. Phys. 18, 4055 (1985); also see references cited therein; J. R. Murray and A. Javan, J. Mol. Spectrosc. 42, 1 (1972).

13. H. M. Goldenberg, D. Kleppner, and N. F. Ramsey, Phys. Rev. 123, 530 (1961).

14. H. G. Robinson and C. E. Johnson, Appl. Phys. Lett. 40, 771 (1982).

16. J. E. Hurst, et al. Phys. Rev. Lett. 43, 1175 (1979).

17. K. C. Janda, et al. J. Chem. Phys. 72, 2403 (1980).

18. J. E. Hurst, et al. J. Chem. Phys. 78, 1559 (1983); 83, 1376 (1985).

19. J. C. Camparo and R. P. Frueholz, Phys. Rev. A 30, 803 (1984).

20. R. B. Brewer, J. Chem. Phys. 38, 3015 (1963).

21. For examples of the use of S_c, the critical speed for trapping, see: B. McCarroll and G. Ehrlich, J. Chem. Phys. 38, 523 (1963); K. Karamcheti and L. B. Scott, Jr., J. Chem. Phys. 50, 2364 (1969), and Ref. 25.

22. J. C. Camparo, J. Chem. Phys, in press.

23. J. C. Camparo, Contemp. Phys. 26, 443 (1985).

24. W. H. Weinberg and R. P. Merrill, J. Vac. Sci. Technol. 8, 718 (1971), and W. H. Weinberg and R. P. Merrill, J. Vac. Sci. Technol. 10, 411 (1973).

25. J. K. Roberts, Proc. Roy. Soc. (London) 129, 146 (1930); D. Menzel and J. Kouptsidis, in Rarefied Gas Dynamics Proceedings of the Ninth International Symposium Vol. 2, Gottingen, 1974, edited by M. Becker and M. Fiebig (DFVLR Press, Porz-Wahn Germany, 1974), p. E.14-1.

26. F. O. Goodman, Prog. Surf. Sci. 5 (3), 261 (1974).

LABORATORY OPERATIONS

The Aerospace Corporation functions as an "architect-engineer" for national security projects, specializing in advanced military space systems. Providing research support, the corporation's Laboratory Operations conducts experimental and theoretical investigations that focus on the application of scientific and technical advances to such systems. Vital to the success of these investigations is the technical staff's wide-ranging expertise and its ability to stay current with new developments. This expertise is enhanced by a research program aimed at dealing with the many problems associated with rapidly evolving space systems. Contributing their capabilities to the research effort are these individual laboratories:

Aerophysics Laboratory: Launch vehicle and reentry fluid mechanics, heat transfer and flight dynamics; chemical and electric propulsion, propellant chemistry, chemical dynamics, environmental chemistry, trace detection; spacecraft structural mechanics, contamination, thermal and structural control; high temperature thermomechanics, gas kinetics and radiation; cw and pulsed chemical and excimer laser development including chemical kinetics, spectroscopy, optical resonators, beam control, atmospheric propagation, laser effects and countermeasures.

Chemistry and Physics Laboratory: Atmospheric chemical reactions, atmospheric optics, light scattering, state-specific chemical reactions and radiative signatures of missile plumes, sensor out-of-field-of-view rejection, applied laser spectroscopy, laser chemistry, laser optoelectronics, solar cell physics, battery electrochemistry, space vacuum and radiation effects on materials, lubrication and surface phenomena, thermionic emission, photosensitive materials and detectors, atomic frequency standards, and environmental chemistry.

Computer Science Laboratory: Program verification, program translation, performance-sensitive system design, distributed architectures for spaceborne computers, fault-tolerant computer systems, artificial intelligence, microelectronics applications, communication protocols, and computer security.

Electronics Research Laboratory: Microelectronics, solid-state device physics, compound semiconductors, radiation hardening; electro-optics, quantum electronics, solid-state lasers, optical propagation and communications; microwave semiconductor devices, microwave/millimeter wave measurements, diagnostics and radiometry, microwave/millimeter wave thermionic devices; atomic time and frequency standards; antennas, rf systems, electromagnetic propagation phenomena, space communication systems.

Materials Sciences Laboratory: Development of new materials: metals, alloys, ceramics, polymers and their composites, and new forms of carbon; nondestructive evaluation, component failure analysis and reliability; fracture mechanics and stress corrosion; analysis and evaluation of materials at cryogenic and elevated temperatures as well as in space and enemy-induced environments.

Space Sciences Laboratory: Magnetospheric, auroral and cosmic ray physics, wave-particle interactions, magnetospheric plasma waves; atmospheric and ionospheric physics, density and composition of the upper atmosphere, remote sensing using atmospheric radiation; solar physics, infrared astronomy, infrared signature analysis; effects of solar activity, magnetic storms and nuclear explosions on the earth's atmosphere, ionosphere and magnetosphere; effects of electromagnetic and particulate radiations on space systems; space instrumentation.

...

END

DATE

FILMED

5-88

DTIC